Embedded Capacitive Displacement Sensor for Nanopositioning Applications

Svetlana Avramov-Zamurovic, *Member, IEEE*, Nicholas G. Dagalakis, *Senior Member, IEEE*, Rae Duk Lee, Jae Myung Yoo, Yong Sik Kim, and Seung Ho Yang

***Abstract*—The scale of nano-sized objects requires very precise position determination. The state-of-the-art manipulators involve accurate nanometer positioning. This paper presents the design, fabrication process, and testing of a capacitance-based displacement sensor. The nanopositioner application required active sensing area dimensions to be hundreds of micrometers, making it necessary to develop sensor electrodes that are a few micrometers in size. The advantages of the sensor presented are its noninvasive method and very low voltage necessary for signal conditioning. Initial results suggest good linearity and sensitivity of 0.001 pF/μm, permitting a reliable displacement resolution on the order of 100 nm.**

***Index Terms*— Capacitance measurement, displacement measurement, fabrication, nano-size positioners, nanotechnology, sensitivity.**

I. Introduction

NANOPOSITIONERS that are equipped with nanoprobes are devices that can precisely manipulate nanoscale objects [1]. State-of-the-art nanopositioners are a few hundreds of micrometers in size. The motion range is less than 50 μm, and the desired step measurement resolution is 1 nm [2]. The 1-nm resolution opens the possibility of controlling nanoscale objects, e.g., nanowires and biological or chemical building blocks. These requirements define motion control law specifications in terms of the system precision and dynamic performance.

One critical component in controlling a nanopositioner motion is a displacement sensor. Due to the size of the devices, the sensor must be fully embedded within the nanopositioning system.

II. Nanopositioner

The Manufacturing Engineering Laboratory, National Institute of Standards and Technology (NIST), Intelligent Systems Division, is developing unique high-precision control and positioning robotic systems for nanoscale dynamic measurements, manipulation, and standards. A planar one-degree-of-freedom (1-DOF) nanopositioner that was constructed at NIST is shown in Fig. 1. This nanopositioner consists of a thermal actuator and a unique platform that is very precisely controlled using an analog proportional–integral controller.

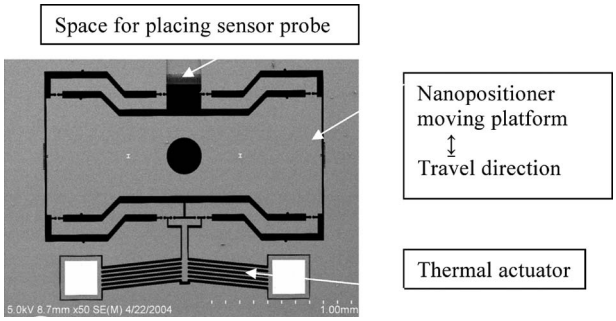

Fig. 1. SEM 2-D picture of the 1-DOF NIST nanopositioner. The space for placing the sensor probe is 300 μm high, 220 μm wide, and 400 μm deep. The nanopositioner moving platform size is 1.8 mm high, 2 mm wide, and 25 μm thick. The thermal actuator is connected to a signal generator. Voltage levels are set to control the current through the actuator chevron beams. The current heats these beams, which, in turn, contract and expand, accordingly moving the platform.

Currently, the capabilities of this device include manipulating a bead with 8-nm accuracy (unpublished test results) and a microelectromechanical system (MEMS) nanorheometer [3]. This rheometer measures the dynamic rheology properties of fluids and soft matter for a desired range of frequencies. Oscillatory strain is produced in a sample sandwiched between the 1-D nanopositioner stage and a glass plate. The resulting stress–strain relationships are obtained by the measurement and analysis of the stage motion. This device can measure test material elastic moduli in the range of 50 Pa–10 kPa over a range of 3–3000 rad/s using less than 5 nL of sample material. This device will provide a new way of characterizing dynamic microrheology of an array of novel materials that will prove useful in a number of areas, including biorheology, microfluidics, and polymer thin films. However, the use of embedded nanodisplacement and nanoforce measurement sensors is critical for its operation. An interdigitated capacitance displacement sensor is under development at NIST. These sensors have very good sensitivity but a limited range of motion due to their finger size. Extending fingers makes them flexible and prone to touching each other. During transient motion, the fingers vibrate and touch, shorting the power supply and destroying themselves. These reasons drive the exploration of

Manuscript received June 12, 2010; revised February 1, 2011; accepted February 3, 2011. Date of publication May 12, 2011; date of current version June 8, 2011. The Associate Editor coordinating the review process for this paper was Dr. Wan-Seop Kim.

S. Avramov-Zamurovic is with the United States Naval Academy, Annapolis, MD 21402-5000 USA (e-mail: avramov@usna.edu).

N. G. Dagalakis, R. D. Lee, J. M. Yoo, Y. S. Kim, and S. H. Yang are with the National Institute of Standards and Technology, Gaithersburg, MD 20899-1000 USA.

Color versions of one or more of the figures in this paper are available online at http://ieeexplore.ieee.org.

Digital Object Identifier 10.1109/TIM.2011.2126150

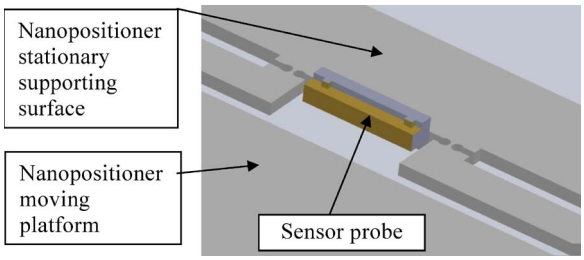

Fig. 2. Computer-aided design (CAD) image of the embedded sensor.

an alternative sensor design as presented in this paper and in [4].

III. Capacitance-Based Displacement Sensor

Most common displacement sensors that are based on capacitance changes involve parallel plate construction, where at least one of the plates is movable [5]. Heerens gave a comprehensive analysis of capacitance sensors and presented design principles to construct a high-resolution multiterminal capacitance sensors [6], [7]. He reported a resolution of 0.12 nm for a motion range of 2.5 mm using the parallel plate structure. He provided design examples that clearly show the superiority of capacitance-based sensing compared to interferometery, thus motivating our research. Current research in MEMS nanometer positioning is focused on parallel plate structures [8] and comb designs [9], [10] that achieve nanometer resolution.

In the case of parallel plate sensors, the capacitance is inversely proportional to the distance between the plates. The change in capacitance directly relates to the displacement measurement with appropriate calibration to account for nonlinearity effects. This idea requires conductive surfaces facing each other and the need to apply the potential difference to both stationary and moving parts. In the case of the NIST nanopositioner, it is difficult to fabricate this type of sensor, because it would require depositing metal electrodes on surfaces hidden deep inside the mechanism trenches.

A. Design

We examined the design of a capacitive sensor using open plates [13]. Planar capacitors are used in tomography, where most of the time, the electrodes are significantly larger compared to the nanopositioner sensor size [12]. In our case, the target object is the movable nanopositioner platform, and the sensor probe is placed on the NIST nanopositioner stationary supporting frame surface, as indicated in Fig 2.

We explored the following design considerations.

1) It is not practical to use the moving platform as one of the capacitor's electrodes; therefore, *a planar capacitor* was designed. Its electrodes, fabricated on a flat surface, create an electric field in which the platform moves.
2) The moving platform is made from doped silicon (conducting material); therefore, measured capacitance changes depend on the distance of the platform from the sensor.

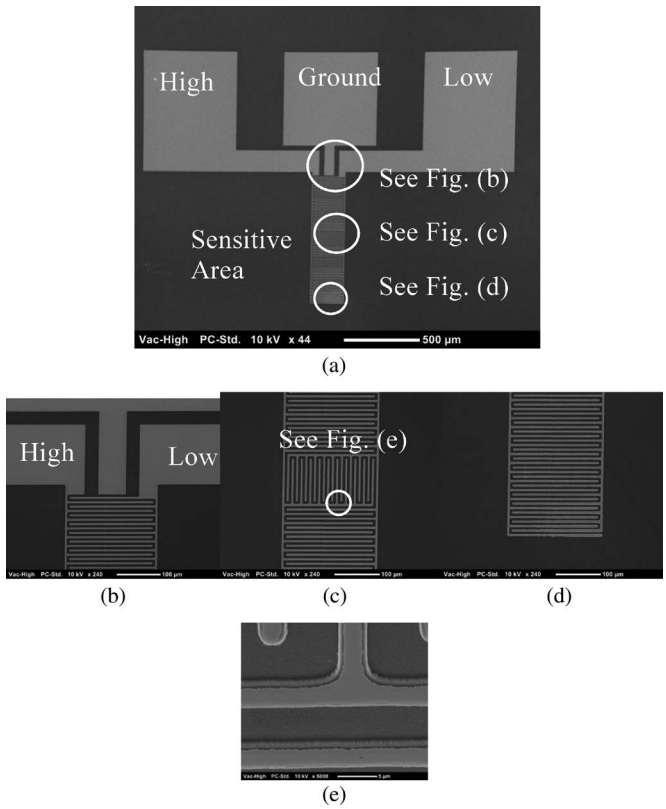

Fig. 3. (a) Overview of the sensor. (b) Top endpoint of the sensitive area. (c) Midpoint of the sensitive area. Note the change in the electrode pattern. (d) Tip of the sensitive area. (e) Enlarged area around the electrodes. This area shows the quality of the electrodes and the gaps fabrication process. The total sensitivity area is $\sim$200 μm $\times$ $\sim$850 μm.

3) The instrumentation for measuring capacitance variations due to platform motion has best sensitivity when measuring 1-pF capacitance. The sensor was designed to have capacitance in the picofarad range.
4) The area where the sensor is placed is small (on the order of hundreds of micrometers); therefore, an electrode pattern has to carefully be designed to have adequate capacitance (around 1 pF).
5) In the case of a planar capacitor, higher capacitance is achieved with longer electrodes, with a small gap between them. This criterion requires packing as many long electrodes as possible on a small area. One practical solution is thin electrodes with narrow gaps between them.
6) The lithography etching process for fabricating the sensor has a resolution limitation that prevented very thin electrode design (smaller than 1 μm).

All of the aforementioned requirements were considered when we explored various capacitor electrodes patterns. The electrode pattern capacitance sensitivity to the movement of the nanopositioning platform was evaluated using a simulation software [4], and the flat comb pattern presented in this paper showed the highest sensitivity. Simulations suggested a possible resolution of 10 nm. In the motion range of 5–10 μm, the simulated capacitance sensitivity was 0.02 pF/μm. Two orientations of the comb fingers were selected for prototype evaluation, as shown in Fig. 3.

The state of the art in measuring 1-pF capacitance when using commercially available bridge instrumentation has a resolution of 0.1 aF, and the measurement uncertainty is five parts in 10^6 at a 4.2-kHz rate [14]. Simulation results suggested that reliable capacitance measurements could be provided if the sensor probe is designed to conform to the optimal measurement range of the bridge. The goal is to have about a 5-aF capacitance change equivalent to a 10-nm displacement. This requirement assumes a good signal-to-noise ratio, a very low sensor probe dissipation factor, a laboratory environment with minimized environmental influences, and well-defined calibration curve, considering that the capacitance–distance relationship is nonlinear. Based on our prototype sensor testing, it is clear that the reliable resolution achieved is on the order of 100 nm. Noise proved to be a major obstacle in achieving a better resolution. A number of strategies are suggested in Section V for overcoming this limitation.

Because the active sensitive area under the platform is very small, to achieve a 1-pF capacitance, the sensor in Fig. 3 was designed with flat comb fingers outside the sensitive area to augment the total measured capacitance, provide structural stability, and allow us the opportunity to explore different patterns at the prototyping phase.

B. Fabrication

The sensor was fabricated using a silicon-on-insulator (SOI) wafer to provide structural stability for easier insertion in the nanopositioner gap. The sensor fabrication steps are shown in Fig. 4. Before depositing a silicon dioxide layer, the wafer was cleaned in a wet chemical cleaning bay in the NIST NanoFab Clean Room, followed by spin rinse drying [see Fig. 4(a)]. A silicon dioxide layer of 0.1-μm thickness was deposited using low-pressure chemical vapor deposition. Then, the top surface of the wafer was coated with 0.05-μm-thick chromium and 0.5-μm-thick gold using an e-beam evaporator. This material is used for our capacitor electrodes. Chromium is deposited to improve the bonding of gold to silicon oxide. Then, the top surface of the wafer was coated with photoresist, which was then exposed to ultraviolet radiation through a mask, using contact optical lithography, and developed. The photoresist mask generates the sensor electrode pattern [see Fig. 4(b)].

Then, the chromium/cold segments, which were exposed by the developed photoresist, were removed using gold and chromium etchants. The exposed silicon dioxide segments were removed using a buffer oxide etch. The removal of the silicon dioxide was very important, because we found that it was responsible for a high dissipation factor when it was left unetched. The final step was to remove the photoresist. This step formed the capacitor electrodes [see Fig. 4(c)].

Following the electrodes and connecting pads etching, the next step was to etch the wafer so that the sensor can be extracted. On the front side, a second mask was used to shape the edges of the sensor. The wafer was spin coated with a microprimer. This step is similar to depositing the layer of chromium before gold. The microprimer helps the photoresist attach to the silicon surface. Then, the photoresist was applied and exposed to ultraviolent radiation according to another mask

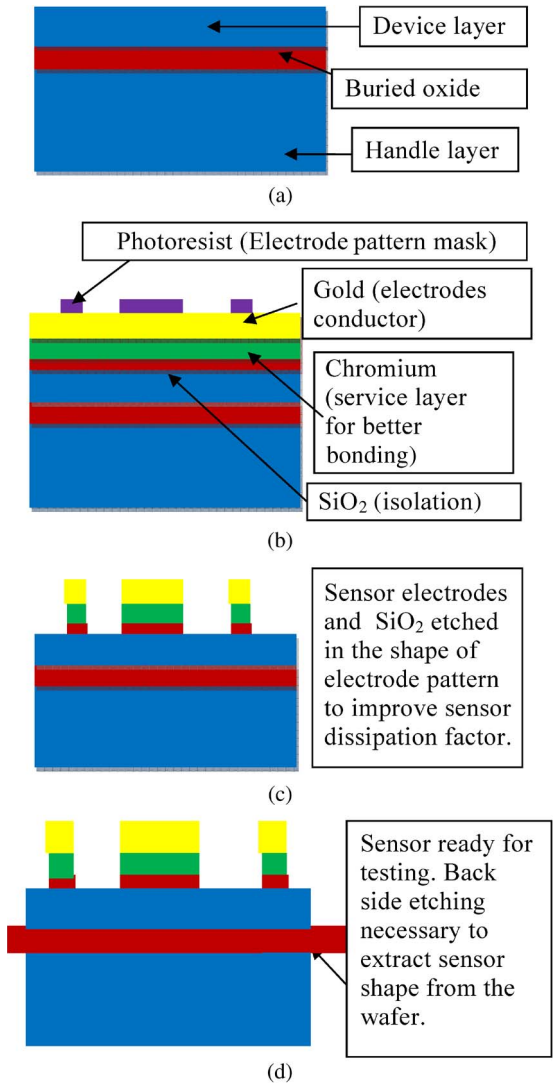

Fig. 4. Sensor fabrication. (a) SOI wafer. (b) SiO_2 was directly deposited on the wafer. The next deposition is Cr as a bond-facilitating layer for Au deposition. The electrode pattern was masked on the top surface using photoresist. (c) Sensor electrodes then formed unnecessary Cr/Au etched. SiO_2 etched in the shape of electrode pattern to improve the sensor dissipation factor. (d) Sensor is ready for testing.

that outlines the edges of the sensor. The photoresist on the wafer went through the optical lithography process and was developed. The wafer front side was then treated with deep reactive ion etching to the depth of the SOI wafer silicon dioxide layer. The next phase was the back side etching for extracting the sensor shape. The steps are similar to the front-side etching [see Fig. 4(d)].

C. Testing

To prepare the test bed for sensor prototype testing, an electric circuit board was designed and fabricated, and a mounting plate was constructed, as shown in Fig. 5. One of the critical issues in capacitive sensing is proper shielding. Because the back-side layer of the sensor is boron-doped silicon with low resistivity, it was connected to the ground pad on the circuit board, providing back-side shielding. The back side of the circuit board is also conductive, where it attaches to the mounting

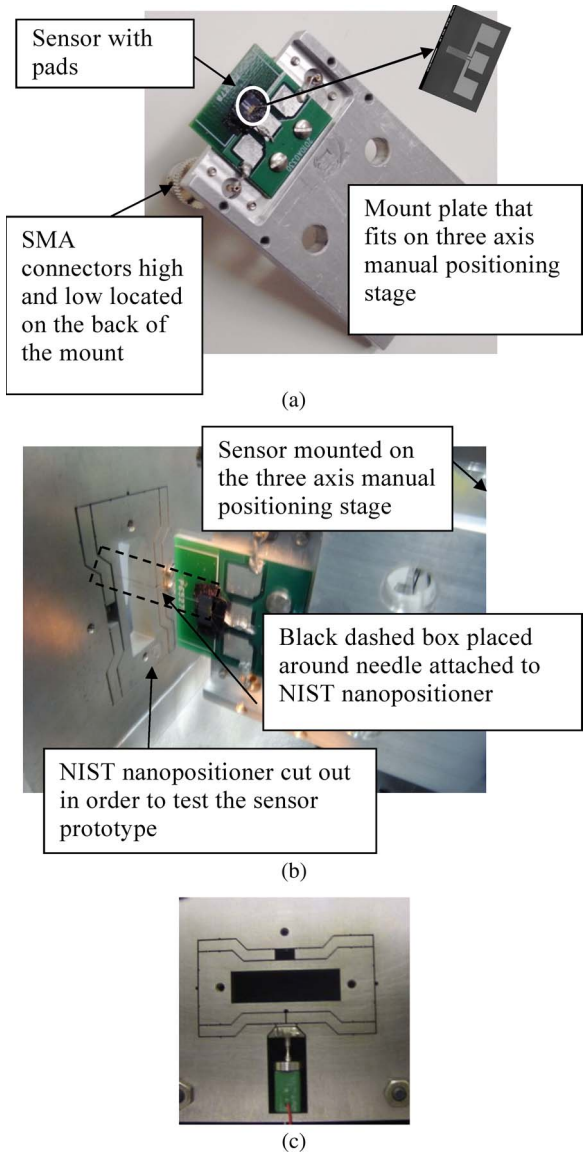

Fig. 5. (a) Sensor on a stage mount. Wire bonding from sensor pads to pads on the circuit broad with a direct link to the subminiature version A (SMA) connectors that lead to the capacitance bridge. (b) Test bed with the NIST nanopositioner. (c) NIST nanaopositioner prepared for testing (the mesoscale nanopositioner).

plate, providing the same ground potential. The circuit board has fitted with two coaxial cables to connect the sensor to the commercial capacitance bridge.

The mounting plate was constructed so that it can be mounted on a three-axis manual positioning stage, which was a commercially available micropositioner. The objective was to position the sensor close to the moving platform using the stage and to keep the sensor stationary. For the sensor prototype testing, a moving surface was held by a larger size nanopositioner [see Fig. 5(c)], which was used to simulate the sensor to placement in the vicinity of the platform. To simulate the sensor operation, a grounded tungsten needle was used to simulate the MEMS platform. This needle had a 150-μm diameter. Fig. 6 shows measuring the capacitance when the moving needle is above the flat electrode comb pattern, with the comb fingers running parallel to the length of the needle.

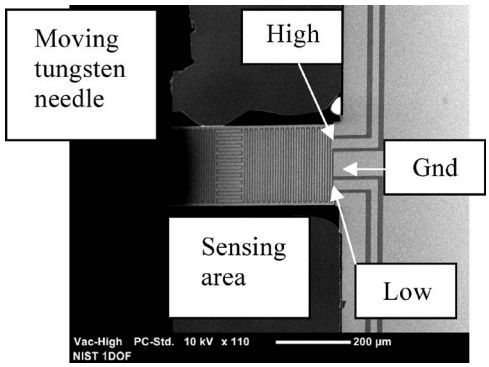

Fig. 6. Moving tungsten needle (150 μm thick) above the sensor. The sensor width is $\sim$200 μm. Note that high and low electrodes change width from $\sim$5 μm in the sensitive area and $\sim$50 μm close to the connector pads. This condition improves the connection quality.

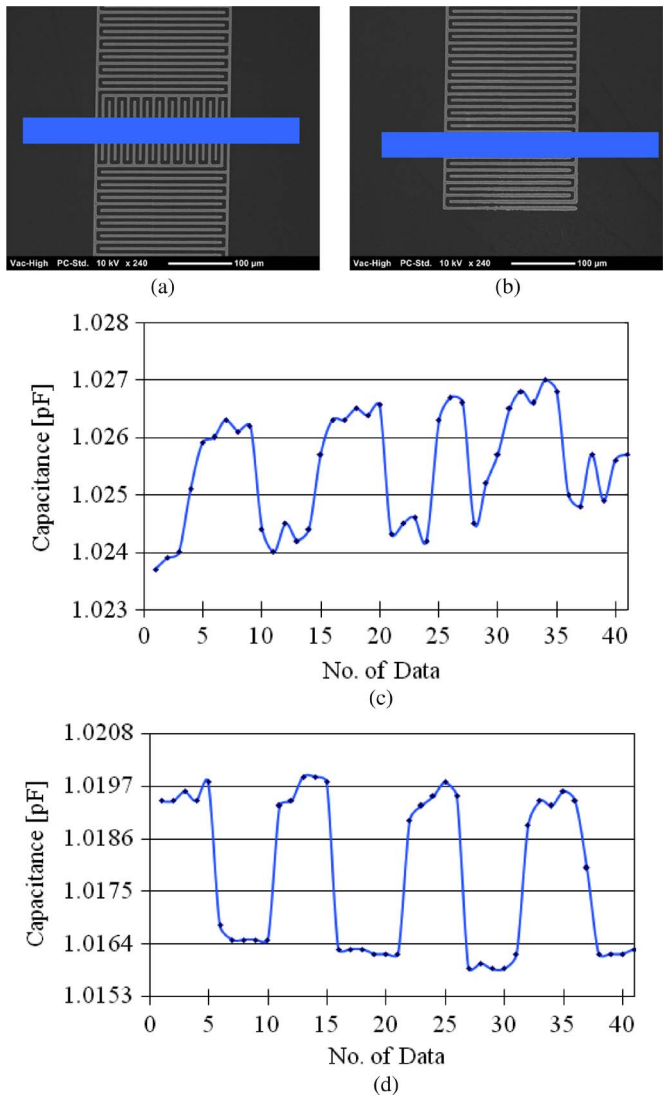

Fig. 7. Sensor was tested using the square-wave function over two different sensing areas. (a) Vertical-pattern sensing area. (b) Horizontal-pattern sensing area. (c) Sensitivity of 0.66 fF/μm over the vertical pattern. (b) Sensitivity of 0.001 pF/μm over the horizontal pattern. Note that the moving object (needle) moved at an average peak-to-peak amplitude of 3 μm. The active sensitive area was $\sim$200 μm $\times$ $\sim$150 μm. Twenty measurements were taken over 1 min with a square-wave function period of 30 s. These tests lasted 2 min.

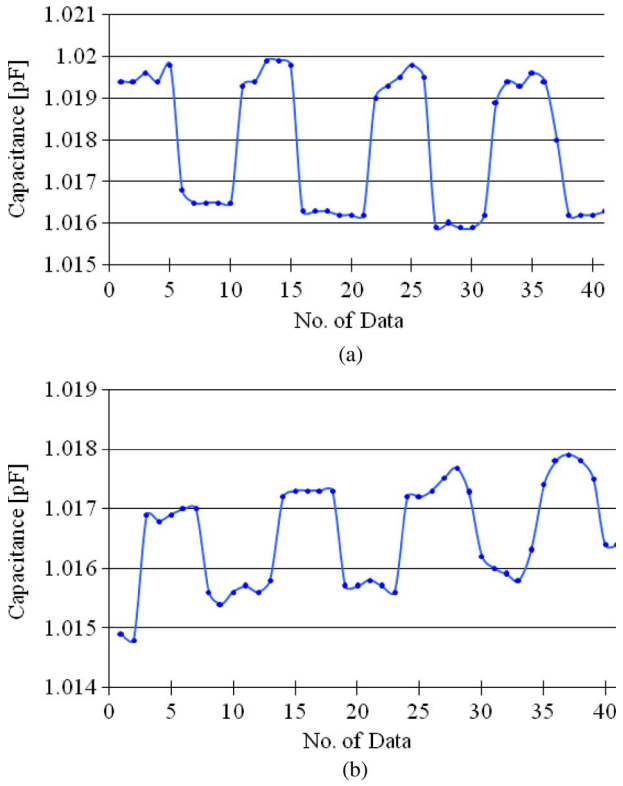

Fig. 8. (a) Motion peak-to-peak amplitude of 3 μm. Sensitivity of 0.001 pF/μm. (b) Motion peak-to-peak amplitude of 1.5 μm. Sensitivity of 0.001 pF/μm. Note the measurements performed over the horizontal pattern sensing area [Fig. 7(b)]. Note the drift of 0.5 fF/min.

IV. Results

During the testing, the sensor was stationary, and the nanopositioner platform moved the needle above it. The motion of the platform was controlled by a signal generator. When a square-wave function was applied, the needle moved from one extreme position to the next in the rhythm of the signal period. The peak-to-peak range was set through the signal amplitude, and the period was set to 30 s to minimize mechanical oscillations and allow capacitance bridge data averaging for better results. The capacitance of the sensor was continuously measured using the capacitance bridge. The bridge applied a 1.5-V signal of 1 kHz to the sensor and averaged 16 samples for each data point, resulting in 20 measurements over 1 min [see Fig. 7(c) and (d)].

The first test looked into the sensitivity of the sensor to the flat comb fingers orientation. The peak-to-peak range of motion was 3 μm. It was observed that the sensor is more sensitive (0.001 pF/μm) over the horizontal pattern [see Fig. 7(a) and (b)] when the needle orientation is horizontal. The tests presented in Figs 8 and 9 were performed using the horizontal pattern.

The next test looked into sensor linearity by changing the peak-to-peak motion amplitude from 3 μm to 1.5 μm. The test results show that the same sensitivity of 0.001 pF/μm was achieved for both amplitudes (see Fig. 8).

The sensor was also tested using sinusoidal and ramp tungsten needle motion (see Fig. 9). Peak to peak amplitude in this test was 3 μm. The measured sensitivity was 0.83 fF/μm.

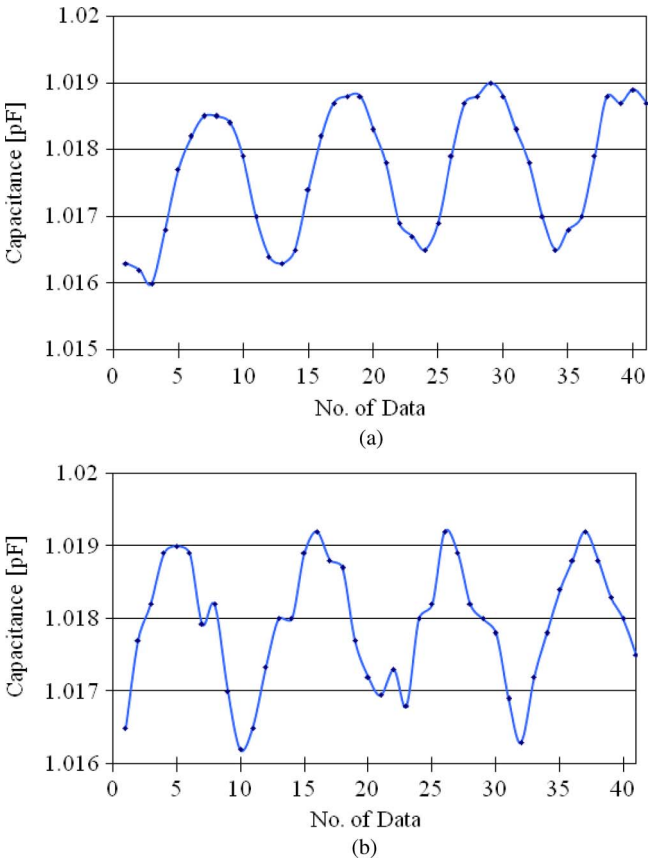

Fig. 9. Motion peak-to-peak amplitude of 3 μm. (a) Sinusoidal motion. (b) Ramp motion.

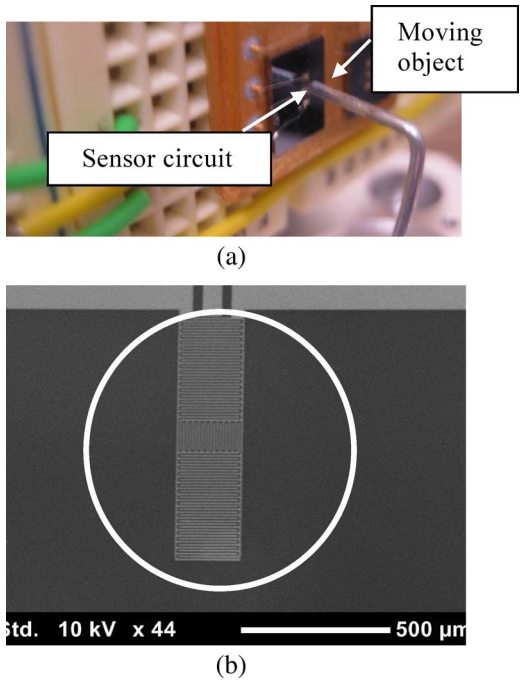

Fig. 10. Sensor testing using a gold-plated magnet as a moving object (with a diameter of 1.2 mm, covering the whole sensing area). (a) Test setup. (b) SEM picture of the sensor with the outline of the moving object.

The sensor performance was also measured using a moving object that covered the whole sensor, instead of only a part of it (see Fig. 10). The object, a gold plated magnet, moved at a

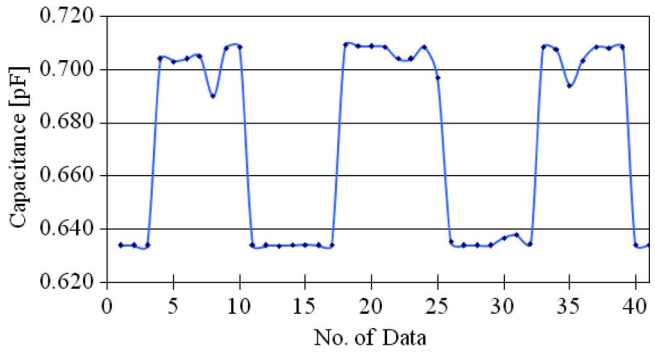

Fig. 11. Sensor sensitivity of 0.018 pF/μm for the setup shown in Fig. 10. The peak-to-peak motion amplitude is 4 μm. The active moving-magnet area in this case is $\sim$200 μm $\times$ $\sim$850 μm.

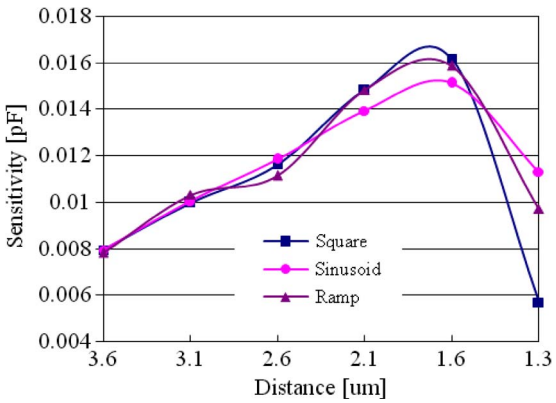

Fig. 12. Sensor sensitivity to the motion of the round object (as given in Fig. 10.) This test was performed for three different actuating signals (square, sinusoid, and ramp, as labeled on the plot). Each data point was obtained by placing the target at a specified distance and then moving it with the peak-to-peak amplitude of 2 μm. Note that the maximum sensitivity of 0.008 pF/μm occurs at a distance of the sensor from the target surface of 1.6 μm. This test was conducted for a target area of $\sim$200 μm $\times$ 850 μm. When this result is compared to the tests given in Figs. 7–9, which have a sensitive area of $\sim$200 μm $\times$ 150 μm, the sensor sensitivities are similar.

peak-to-peak amplitude of 4 μm. The results show a sensitivity of 0.018 pF/μm (see Fig. 11). Note that the active sensitivity area in this case is $\sim$200 μm $\times$ $\sim$850 μm.

Because this configuration showed very good performance, we measured the sensor response for three different actuating signals. The sensor response sensitivity and linearity to different inputs were consistent. Fig. 12 shows the sensor sensitivity as a function of the sensor to moving surface average distance. The graph shows that the sensitivity peaks at a distance of 1.6 μm. It is obvious that the next design iteration will have to try to extend the peak performance to a larger range.

The sensor repeatability in the active regime is a measure of the measurement uncertainty. A square-wave motion was applied to a 700-μm-diameter tungsten needle in front of the sensor. For each data point in Fig. 13, 41 measurements were taken, and the average capacitance and standard deviation were plotted. The standard deviation is the estimate of the measurement noise. Assuming a sensitivity of 0.001 pF/μm, a standard deviation of 0.1 fF corresponds to a displacement resolution of 100 nm. The sensor was tested for over 44 min, and the drift was measured to be 0.1 fF/min. This calculation estimates the sensor and target actuator long-term stability in the active mode.

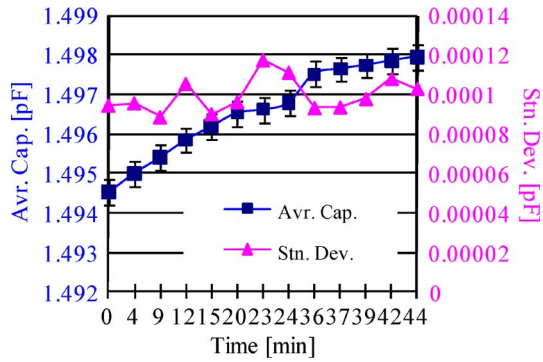

Fig. 13. Sensor repeatability in the active operating mode. The sensor was tested using a 700-μm-diameter needle as a moving target object actuated by a square-wave signal with a period of 20 s. The target peak-to-peak motion amplitude was 4 μm. The test took 44 min. Forty-one measurements were taken at each data point to calculate the standard deviation. The length of the bars represents the range between the maximum and minimum capacitance measured values.

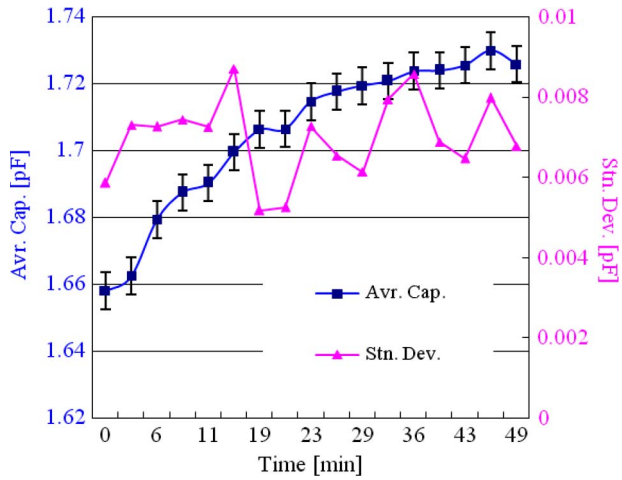

Fig. 14. Sensor stability test in the passive operating mode. The sensor capacitance was measured over 49 min without a moving target object in the sensing area. Each measurement point on the plot is an average capacitance calculated using 40 readings. For each data point, the standard deviation was calculated. The length of the bars represents the range between the maximum and minimum capacitance measured values.

The sensor drift was measured over 49 min without any target motion (see Fig. 14). The measurements and calculations were exactly performed the same way as in the previous test (see Fig. 13). The results show the long-term stability of the sensor alone in the passive operating mode of 0.001 pF/min. The standard deviation for each data point is less than 0.008 pF. This result points to the limit in the performance of the sensor. One possible source of this drift could be the low thermal conduction coefficient of the material that was used for the sensor fabrication, poor wiring connection, or bridge instrument drift.

V. Discussion

Preliminary tests demonstrate an encouraging sensitivity of 0.001 pF/μm, with a noise estimate of 0.1 fF, allowing the possibility of reliable displacement resolution better than 100 nm.

The following issues were observed during the development and testing, which will be addressed in the second iteration.

1) *Stability*. Measurements show a significant drift in the active and passive modes of operation. The measurements were made in laboratory conditions, but the environment was not controlled. To perform micrometer motion, a number of microscopes and their illuminating lights were used, resulting in heating the sensor. These effects will be minimized in the final design by the use of a "dummy" sensor built on the same silicon wafer and shielded from detecting platform motion. The next iteration of the displacement sensor can include "active" and "passive" sensors for environmental influences compensation.
2) *Noise*. The noise level measured is not acceptable for nanometer displacement control. One of the main contributions to the high noise level is a possible connection from the sensor active area to the capacitance bridge instrument. Wire bonding was used to connect the sensor pads to the breadboard. The breadboard is coaxially connected to the capacitance bridge. Wire bonding proved to be the most critical step in sensor development, because it required extra effort to make reliable and repeatable connections. When the connections were done well, the capacitance bridge operated on the order of six digits of resolution, providing ample reliability for the results. Improved electrical connections are necessary to reduce the noise level and achieve stability, which is necessary to establish good calibration uncertainty.
3) *Dissipation factor*. Because this sensor is built on a silicon wafer and silicon oxide is used for the isolation layer, the dissipation factor is measured to be 0.1 (value of measured loss expressed as a unit less number) [14]. As the first step to minimize the dissipation, we changed the fabrication steps by etching both gold electrodes and silicon oxide between the electrodes. In this case, a smaller portion of the field propagates through a low-performance material (e.g., silicon oxide). The drawback of this step is the possibility of moisture condensing in the created gaps between the electrodes, increasing the humidity factor and deteriorating the measurements. This effect will closely be monitored in the next iteration.

   As an alternative step, an exterior circuit board that consists of resistors and capacitors was explored to reduce the value of the dissipation factor. This circuit board, which houses the sensor mounting, will be modified to allow for connecting the dissipation compensation circuit. A software program has been developed to find values of resistors and capacitors to eliminate the dissipation factor. This option will be used in the next design cycle.
4) *Simulations*. Comprehensive simulations have to be developed to reflect the true fabrication process and thus produce displacement–capacitance characteristics useful for sensor calibration.

VI. Conclusion

A capacitance-based displacement sensor has been developed for a nanopositioning application. Preliminary results show good linearity while measuring the square-wave, sinusoidal, and ramp motions of the target object. A sensitivity of 0.001 pF/μm, with an estimated uncertainty of 0.1 fF, was achieved while measuring the peak-to-peak motion with a range of several micrometers above the active sensitive area of 200 μm $\times$ 150 μm. Measurements were made at a 1-pF level with a driving voltage of 3 V. Low measuring voltage is beneficial in nanotechnology, because it has low impact on circuit structures that are fragile. The measured sensitivity result is encouraging, because the capacitance bridge that was used in this application has a resolution of 0.1 aF, allowing a capacitance-based displacement sensor sensitivity of less than a 1-nm resolution. For this result, significant improvements have to be made to reduce the measurement noise.

Acknowledgment

The authors would like to thank Mr. B. Waltrip of the National Institute of Standards and Technology (NIST) for the ongoing help on the project through constructive discussions and for providing essential instrumentation and software support and Mr. R. Palm of NIST for the most extraordinary technical support.

References

[1] J. J. Gorman, Y. S. Kim, A. E. Vladar, and N. G. Dagalakis, "Design of an on-chip microscale nanoassembly system," *Int. J. Nanomanufacturing*, vol. 1, no. 6, pp. 710–721, 2007.
[2] J. J. Gorman, Y. S. Kim, and N. G. Dagalakis, "Control of MEMS nanopositioners with nanoscale resolution," presented at the ASME Int. Mechanical Engineering Congr. Expo. (IMECE), Chicago, IL, Nov. 2006, IMECE2006-16190.
[3] G. F. Christopher, N. G. Dagalakis, S. D. Hudson, and K. B. Migler, "MEMS parallel-plate rheometer for small-amplitude oscillatory shear microrheology measurements," presented at the Society Rheology 81st Annu. Meeting, Madison, WI, Oct. 18–22, 2009.
[4] S. Avramov-Zamurovic, N. G. Dagalakis, R. D. Lee, Y. S. Kim, J. M. Yoo, and S. H. Yang, "Embedded capacitive displacement sensor for nanopositioning applications," in *Proc. CPEM*, Daejeon, South Korea, Jun. 2010, pp. 316–317.
[5] L. K. Baxter, *Capacitive Sensors*. Piscataway, NJ: IEEE Press, 1997.
[6] W. C. Heerens, "Multiterminal capacitor sensors," *J. Phys. E: Sci. Instrum.*, vol. 15, no. 1, pp. 137–141, Jan. 1982.
[7] W. C. Heerens, "Application of capacitance techniques in sensor design," *J. Phys. E: Sci. Instrum*, vol. 19, no. 11, pp. 897–906, Nov. 1986.
[8] Y. Ma, Z. Zhang, and L. Gao, "Research of thick-film capacitive displacement sensors used in nanometer scaled operation," in *Proc. 3rd IEEE Int. Conf. NEMS*, 2008, pp. 90–94.
[9] W. Merlijn van Spengen and T. H. Oosterkamp, "A sensitive electronic capacitance measurement system to measure the comb drive motion of surface micromachined MEMS devices," *J. Micromech. Microeng.*, vol. 17, no. 4, pp. 828–834, Apr. 2007.
[10] X. Liu, J. Tong, and Y. Sun, "Millimeter-sized nanomanipulator with subnanometer positioning resolution and large force output," in *Proc. 7th IEEE Int. Conf. Nanotechnol.*, 2007, pp. 454–457.
[11] A. Kuijpers, R. J. Wiegerink, G. J. M. Krijnen, T. S. J. Lammerink, and M. Elwenspoek, "Capacitive long-range position sensor for microactuators," in *Proc. 17th IEEE Int. Conf. MEMS*, 2004, pp. 544–547.
[12] A. Somerville, I. Evans, and T. York, "Preliminary studies of planar capacitance tomography," in *Proc. 1st World Congr. Ind. Process Tomography*, Buxton, U.K., 1999, pp. 522–529.
[13] S. Avramov-Zamurovic and R. D. Lee, "A high-stability capacitance sensor system and its evaluation," *IEEE Trans. Instrum. Meas.*, vol. 58, no. 4, pp. 955–961, Apr 2009.
[14] *AH 2550A Ultraprecision Capacitance Bridge Manual*, Andeen-Hagerling, Cleveland, OH. [Online]. Available: http://www.andeen-hagerling.com

Svetlana Avramov-Zamurovic (M'97) received the B.S. and M.S. degrees in electrical engineering from the University of Novi Sad, Novi Sad, Serbia, in 1986 and 1990, respectively, and the Ph.D. degree in electrical engineering from the University of Maryland, College Park, in 1994.

Since 1990, she has been a Guest Researcher with the National Institute of Standards and Technology, Gaithersburg, MD. She is currently a Professor with the United States Naval Academy, Annapolis, MD. Her recent work with NIST involves the development of impedance-measuring techniques and designing and building displacement sensors for various applications, including nanopositioning. At the Academy, she is currently involved in research on laser beam propagation in the maritime environment.

Nicholas G. Dagalakis (SM'10) received the M.S., Eng.D., and Ph.D. degrees from the Massachusetts Institute of Technology (MIT), Cambridge, and the Diploma degree in mechanical and electrical engineering from the National Technical University of Greece, Athens, Greece.

He has been with two small companies, with MIT as a Research Associate, and with the University of Maryland, College Park, as an Assistant Professor. In 1985, he joined the National Institute of Standards and Technology (NIST), Gaithersburg, MD, as a full-time Research Staff. He has conducted research in electrical generation, biomedical engineering, robotics, high-precision micromanufacturing/nanomanufacturing, sensors, and standards. Since 1999, he has been a Project Leader for several NIST- and other agency-funded projects. He is the author or a coauthor of 25 journal papers, 51 conference proceedings papers, four reports, and two books. He is the holder of two patents.

Dr. Dagalakis is the recipient of the 2008 U.S. Senate Special Committee on Aging Award and the 2009 NIST Bronze Medal Award.

Rae Duk Lee received the B.S. and M.S. degrees from Soong-Jun University, Daejeon, Korea, in 1968 and 1980, respectively, and the Ph.D. degree in physics from Han-Nam University, Daejeon, in 1991.

In 1978, he joined the Electricity Laboratory, Korea Research Institute of Standards and Science (KRISS), Daejeon, from which he retired in 2006. He then became a Guest Researcher with the National Institute of Standards and Technology (NIST), Gaithersburg, MD. He has been working on the development of impedance standards and capacitive sensors at low frequency. He is currently with NIST, working on the development of a next-generation calculable cross capacitor.

Jae Myung Yoo received the M.S. and Ph.D. degrees in mechanical engineering from the Chung Ang University, Seoul, Korea, in 2000 and 2006, respectively.

He is currently a Research Associate with the National Institute of Standards and Technology, Gaithersburg, MD. His research activity is mainly focused on microelectromechanical systems with sensors. His research interests include medical robots and medical sensors.

Yong-Sik Kim received the M.S. degree in mechanical engineering from the Korea Advanced Institute of Science and Technology (KAIST), Daejeon, Korea, in 2004. He is currently working toward the Ph.D. degree at the University of Maryland, College Park.

He is currently a Research Associate with the National Institute of Standards and Technology, Gaithersburg, MD. His research activity is mainly focused on the design, testing, and optimization of MEMS nanopositioners, MEMS microforce, and nanodisplacement sensors.

Seung Ho Yang received the M.Sc. and Ph.D. degrees in mechanical engineering from the Yonsei University, Seoul, Korea, in 1998 and 2002, respectively.

From 1991 to 1998, he was with Samsung, Korea. From 1994 to 1996, he was involved in a joint research project between Samsung and the Russian Academy of Science. From 1996 to 2002, he was with the Korea Institute of Science and Technology (KIST). He is currently a Research Associate with the National Institute of Standards and Technology, Gaithersburg, MD. He has been a Reviewer of peer-reviewed journals, including *Nanotechnology*, *Journal of Micromechanics and Microengineering*, *Measurement Science and Technology*, *Journal of Physics D*, *Philosophical Transactions of the Royal Society A*, and *Sensors and Actuators A*. He is a coauthor of 28 scientific papers and 39 conference proceedings. He is a coholder of six patents. His research interests include nanomechanics, microelectromechanical systems, and tribology.

Dr. Yang is an Affiliated Member of the American Society of Mechanical Engineers (ASME). He received the bronze medal for Samsung's New Technology Award in 1996 and the KIST Academic Excellence Award in 2002. He received a Postdoctoral Fellowship from the Korean Government (Korean Science and Engineering Foundation) in 2002.